Memristive Switching: From Individual Nanoparticles Towards Complex Nanoparticle Networks

Niko Carstens, Maik-Ivo Terasa, Pia Holtz, Sören Kaps, Thomas Strunskus, Abdou Hassanien, Rainer Adelung, Franz Faupel, and Alexander Vahl

Abstract Novel hardware concepts in the framework of neuromorphic engineering are intended to overcome fundamental limits of current computer technologies and to be capable of efficient mass data processing. To reach this, research into material systems which enable the implementation of memristive switching in electronic devices, as well as into analytical approaches helping to understand fundamental mechanisms and dynamics of memristive switching is inevitable. In this chapter, memristive switching based on Ag metal filament formation is discussed throughout different scales, providing insights on the stability of metal filaments and the onset of collective behaviour. An unconventional cAFM approach, which intends to integrate the memristive system directly on the apex of the cantilever instead of usual contacting is presented. This facilitates the nanoscale probing of filamentary memristive switching dynamics on long time scales for the purpose of basic research, which is demonstrated by an archetypical electrochemical metallization (ECM) based system consisting of $Ag/Si_3N_4/Au$. Further, the application of AgAu and AgPt noble metal alloy nanoparticles (NPs) for memristive devices is discussed with special focus on the device scalability. For the smallest scale it is shown, that a single AgPt-NP encapsulated in SiO_2 operates via stable diffusive switching. Finally, two concepts for the self-assembled fabrication of NP-based memristive switch networks are evaluated regarding to collective switching dynamics: A sub-percolated CNT network decorated with AgAu-NPs and a Ag-NP network poised at the percolation threshold. The hybrid CNT/AgAu-NPs networks exhibit a mixed form of diffusive and bipolar switching, which is very interesting for tailoring the retention time, while

N. Carstens · T. Strunskus · F. Faupel · A. Vahl (✉)
Institute for Materials Science, Kiel University, Chair for Multicomponent Materials, Kaiserstr. 2, 24143 Kiel, Germany
e-mail: alva@tf.uni-kiel.de

M.-I. Terasa · P. Holtz · S. Kaps · R. Adelung
Institute for Materials Science, Kiel University, Chair for Functional Nanomaterials, Kaiserstr. 2, 24143 Kiel, Germany

A. Hassanien
Department of Condensed Matter Physics, J. Stefan Institute, Jamova 39, 1000 Ljubljana, Slovenia

the networks dynamics of percolated Ag-NP networks are governed by ongoing transitions between a multitude of metastable states, which makes them interesting for reservoir computing and other neuromorphic computation schemes.

Keywords Memristive devices · Diffusive switching · Self-assembled networks · Nanoparticles · Neuromorphic engineering · Dynamic networks

1 Introduction

For several decades, the increasing demand for computational data processing was satisfied by miniaturization of the transistor, which plays the role of the fundamental building unit in modern computer technology, through extreme manufacturing techniques and engineering of materials. Alongside with current developments like Internet of Things or autonomous driving for which massive data processing is required, the demand for computational power presumably cannot be met by conventional computer technologies in the near future [1]. One reason for this relates to physical limits as the size of a single transistor approaches atomic scale like a fundamental integration density limit or information lost via inadvertent tunneling currents [2]. Another reason is the strict separation of information processing and storage units predefined by the von-Neumann architecture of modern computer systems, since the duration for massive data transfer between both units evolved into a bottleneck. In foreseeable future, a gap in the computer technology must be filled in order to remain capable of dealing with an increasing massive amount of data. The field of neuromorphic engineering comes along with unconventional computation schemes, which aim to overcome the aforementioned limits by implementation of biological computation principles in novel kind of hardware [3, 4]. Memristive devices play a fundamental role in the realization of bio-inspired hardware. They are two-terminal passive circuit elements, whose internal state (represented by the resistance of the device) is sensitive to external voltage or current stimuli [5]. This property allows the implementation of key features for neuromorphic computation like parallelism, in-memory computing and plasticity [2]. Moreover, the functionality of memristive devices can be expanded towards memsensing, which means a combination of memristive and sensitive properties [6]. Tremendous work was dedicated to the development of material systems showing memristive behavior and understanding of nanoscale processes which are responsible for the memristive switching property, which resulted in a multitude of memristive material systems exhibiting diverse memristive switching dynamics [7]. One example is analog non-volatile switching, which is a potential electrical characteristic for long-term memory in neuromorphic circuits and enables the hardware implementation of artificial neural networks. Diffusive switching possesses a volatile threshold-like dynamic beneficial for short-term memory realization and incorporation of non-linearity in neuromorphic circuits, which are both inherent for brain functionality [8, 9].

Besides valence change [10] and phase change mechanisms [11], the electrochemical metallization (ECM) is of special interest to engineer materials with memristive properties. ECM relies on redox-reactions and ion transport of active metallic species, like Ag or Cu, in a nanoscale switching gap upon application of an external electrical field [12]. The switching dynamics in ECM devices is dominated by the reconfigurable formation and rupture of a thin filament composed of the active metallic species. The operation of ECM devices can be constrained into a diffusive regime by utilization of a strict limitation of current flowing through the device during its operation or by limiting the amount of the active metallic species [13]. The understanding and control of the complex processes governing the filament evolution during device operation is still a current challenge. Especially, the inherent stochasticity in the switching dynamics (in terms of variation of switching voltages from cycle to cycle) is merely insufficiently studied. The stochasticity may impede the development of certain applications like selector devices, but it may also be exploited like in the design of true random number generators [14, 15].

A critical issue in the development of neuromorphic hardware is the challenge of upscaling from individual memristive units to networked assemblies with an enormous degree of complexity. Promising approaches under circumvention of vast wiring procedures rely on self-assembly of memristive switching units. Reports have shown, that nanoparticles (NPs) of Au [16, 17] or Sn [18] or Ag-nanowires [19, 20] can be applied as fundamental memristive building units for self-assembled networks. Such networks are capable of responding via complex dynamical switching patterns featuring short-term memory and temporal correlations, which are both key requirements for concepts like reservoir computing [21]. A feasible strategy to maximize the degree of complexity in self-assembled networks of switching units, and therefore to approach neural complexity, is to make use of criticality, where the network dynamics are governed by complex correlated patterns, similar to those observed in neural tissues [22, 23]. Networks of memristive switching units can be operated at critical dynamics, when the connectivity inside the system is poised at the percolation transition [24]. Developments in the design of material systems and deeper characterization of emergent properties in networks of memristive units could be a significant advancement for bio-inspired computation strategies.

In this chapter, we discuss basic studies on Ag-based filamentary switching and approaches for device implementation on fundamentally different scales, ranging from single switching junctions to complex network behavior. Firstly, an unconventional conductive atomic force microscopy (cAFM) approach giving deep insights into the long-term switching dynamics and inherent stochasticity of a single Ag-filament is presented. Moreover, the application of Ag-based bimetallic noble metal NPs as individual memristive switching units is discussed. Major emphasis is put on implications which arise, when the memristive system is scaled up from a single switching unit towards macroscopic assemblies of switching units, i.e. up to which scale does the characteristics of individual NPs retain and when does collective behavior emerge. Therefore, discussions on macroscopic assemblies realized by two different approaches in which Ag-based noble metal NPs are incorporated into complex networks are given in the last section: The first approach comprises a

randomly assembled CNT network with Ag-based NPs as localized switching units while the second approach involves self-assembled networks of Ag-NPs poised at the percolation threshold.

2 Deep Insight into Single Filament Switching Via an Unconventional cAFM Approach

Progress in the development of novel neuromorphic hardware is directly reliant on the understanding of the fundamental units causing the memristive action. In ECM-based devices, as well as in self-assembled memristive switch networks, this fundamental unit is a single metallic filament, which defines an either conductive (low resistive state, LRS) or insulating (high resistive state, HRS) state of a nanogap. In ECM-based devices, there is in most cases solely one single filament, which dominates the behavior of the whole device [25]. Considering the typical diameter of an active filament in the order of 10 nm, this means that all memristive action during device operation takes place highly localized on the nanometer scale and is independent of the devices' geometrical dimensions defined through the fabrication [26]. The analysis of inherent stochastic features in the switching dynamics of single filaments are of special interest, because they set fundamental constraints on possible applications. On the contrary, in self-assembled memristive switch networks, filamentary switching is spatially distributed over a huge number of nanogaps throughout the network and the network response results from a complex interplay between the states of different filaments. In such networks, studies on single filamentary switching are likewise inevitable to understand the role of single elements in the collective network dynamics.

CAFM raised to an essential tool probing electrical properties on the nanoscale and was commonly used to make localized studies on switching filaments [27]. However, a prominent drawback of the conventional cAFM method is associated to the thermal drift of the cantilever, because it imposes uncertainties regarding the position of the cantilever relative to the filament under investigation. The extent of the thermal drift is usually more than 10 nm h^{-1}, which exceeds the typical dimensions the filament. This is especially problematic when the long-term electrical response of a single filament shall be measured. To circumvent this issue, an unconventional cAFM approach to probe the long-term response of the memristive switching of a single filament can be applied [28]. Instead of conventional contacting, the memristive device is integrated directly on the apex of a conductive cantilever. In this way, the functionalized cantilever can be brought in reliable contact using the cAFM instrumentation to any surface which acts as an inert counter electrode. This approach is sketched in Fig. 1.

Archetypical memristive systems consisting of a few nm thin Ag layer covered by a dielectric layer on Si_3N_4 were deposited on the apex of cantilevers by conventional physical vapor deposition (PVD) techniques. The basic coating of the cantilever
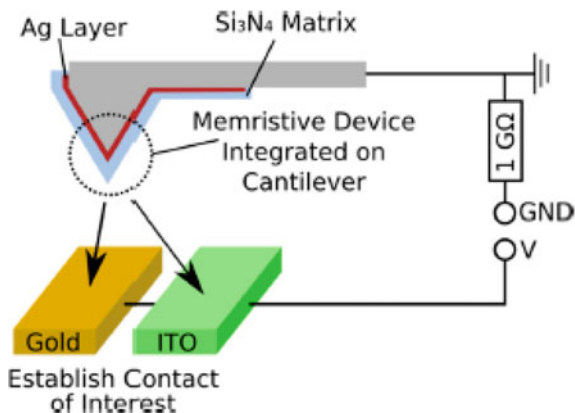
Fig. 1 Unconventional cAFM approach in the present study. Instead of conventional contacting, the memristive system is integrated on the apex of the cantilever via PVD methods. The functionalized cantilever is brought into contact with inert counter electrode surfaces (Au and ITO in this work) resulting in an ECM-based memristor configuration. As the filamentary switching is directly constrained to the apex, this approach allows more reliable long-term measurements on the nanoscale via conventional cAFM instrumentation. Reproduced under CC-BY 4.0 license from [28]

was chosen as Au to guarantee a good conductivity and electrochemical passivity of the cantilever. The configuration of functionalized cantilever contacted to the inert counter electrode surface defines a complete ECM-device to be probed. Cantilevers functionalized with Ag/Si_3N_4 were investigated under two different configurations: Having either Au or indium tin oxide (ITO) as inert counter electrode. This approach offers two decisive advantages for the purpose of basic research. Firstly, the memristive action through the filament is constrained directly to the apex of the cantilever. Consequently, thermal drift causing lateral motion of the cantilever over the counter electrode surface does not lead to any separation of probe and switching locality. As thermal drift effects are mitigated, reliable nanoscale long-term measurements of the filamentary switching activity are enabled using conventional cAFM instrumentation. Another advantage of this approach concerns the flexibility in choosing the experimental configurations, because an identical functionalized cantilever can be brought into contact to diverse counter electrodes. This enables strategies to investigate the switching activity of the very same filament on different interfaces.

In the following, the long-term switching of a single filament is discussed based on data gathered from a cantilever functionalized with Ag/Si_3N_4 contacted to a Au surface. The contact was held at a well-controlled force of 1.2 nN to provide non-invasive measurement conditions. The counter electrode was biased via voltage sweeps between −2.6 and 2.6 V and current responses were recorded continuously over 18 h resulting in over 12,000 switching cycles. During the measurement a 1 GΩ serial resistance was applied to limit the current and protect the cantilever

from Ag over-diffusion. The filamentary switching mechanism taking place sharply localized at the apex and an exemplary switching cycle are shown in Fig. 2a and 2b, respectively. Initially, under zero-bias conditions, the sample is in its HRS since no stable filament can exist between probe and counter electrode. Upon biasing the counter electrode (towards either polarity), electrochemical oxidation of Ag is triggered at anodic sites in the sample, leading to a release of Ag^+ -ions into the dielectric layer. The Ag^+ -ions are mobile and can migrate in the Si_3N_4 layer until they become reduced at cathodic sites in the sample where they aggregate as metallic silver. Through this mechanism, metallic Ag is reconfigured in the dielectric layer until a continuous filament bridges the Si_3N_4 layer, which causes a switching event to the LRS. This moment is denoted as a SET event in the current response and the current level (highlighted in blue) is solely limited by the external 1 GΩ serial resistance. When the voltage bias is reduced coming from the LRS, a RESET event is observed before reaching zero-bias. The physical mechanism behind this is the spontaneous disintegration of the Ag filament into individual clusters caused by interface energy minimization [13]. The fact that the filament is only stable above a certain threshold voltage is the most prominent feature of diffusive memristive switching. Among all cycles in the long-term measurement, 95% of them showed clear diffusive switching, which indicates the stable and non-invasive measurement conditions of this approach. It should be noted, that the incorporated 1 GΩ resistance is the reason why the switching is constrained into the diffusive regime. On the one hand side, the limited current only allows for the formation of thin filaments which are more prone to spontaneous disintegration. On the other hand, in the moment of SET switching the major part of the externally applied electrical potential shifts to the serial resistor, which significantly reduces the field across the filament.

In another experiment, the consequences of having Au or ITO as counter electrode interface are investigated. For this purpose, the Ag/Si_3N_4 system of an identical cantilever was brought into contact firstly with Au and subsequently with ITO. The decisive advantage of this approach is that an identical active filament was probed in consecutive measurements under different ECM-based device configurations. Therefore, all influence coming with the active electrode or dielectric layer (such as defect structure or filament morphology), which might disturb the comparability of different configuration, are ultimately kept constant. In contrast to that, in conventional cross-point devices, an investigation of the variation of different counter electrodes is only possible at the expense of losing the direct comparability in terms of the exact same filament [29, 30]. Figure 2c depicts the current response during operation on Au (black) and ITO (red) over 50 consecutive cycles for each electrode. It can be seen that interfacing to Au drives the switching window to lower voltages. A representative switching cycle (scan speed: 4 s per cycle) drawn in bold line shows a switching window between a RESET voltage of 0.3 V and a SET voltage of 1.9 V in the positive regime. Further, it was detected that upon interfacing to Au the LRS follows a linear characteristic, which reveals that contact between filament and counter electrode surface is purely ohmic. Switching the contact to ITO in the subsequent measurement resulted in fundamentally different electrical characteristics. In this configuration, the switching window is shifted to higher voltages (above
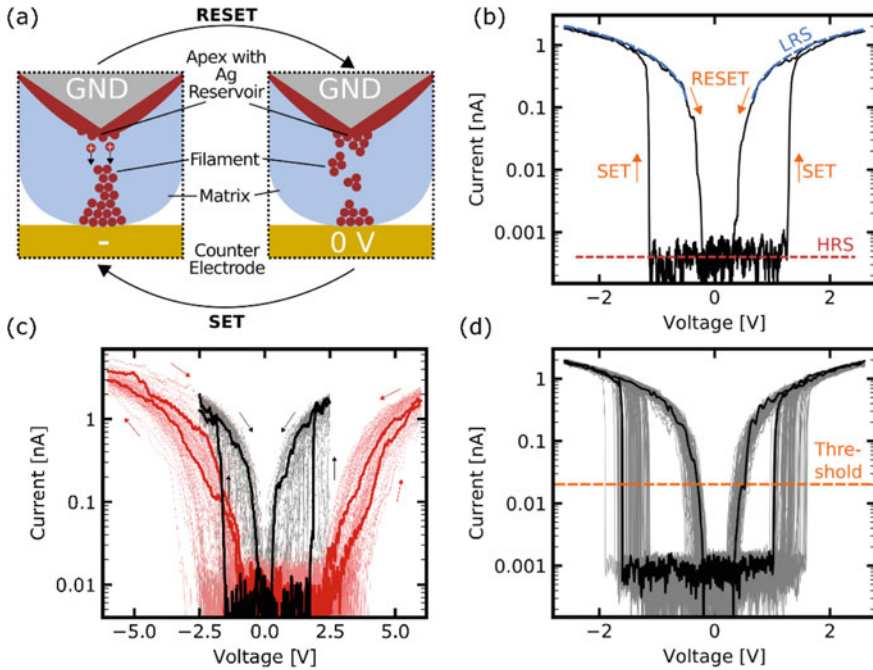
Fig. 2 a Physical mechanisms taking place during filamentary switching in the sample. **b** Representative cycle from the long-term measurement. The operation of the Ag/Si$_3$N$_4$ system integrated on a cantilever and contacted to a Au surface resulted in diffusive switching characteristics due to the 1 GΩ serial resistance. The distinctive feature of diffusive switching is, that the LRS is only stable above a certain threshold voltage and volatile at zero-bias conditions. **c** Operation of an identical filament from one functionalized cantilever on different counter electrode surfaces: Au (black) and ITO (red). A non-linearity in the current response was detected for ITO, which indicates the existence of an energetic barrier which was not observed during operation of the very same filament on Au. **d** Representation of 100 consecutive cycles among the long-term measurement. It can be seen, that SET and RESET threshold voltages have a statistical nature. Reproduced under CC-BY 4.0 license from [28]

2.5 V in the positive regime) and the current–voltage dependency exhibited a strong non-linearity. This indicates the occurrence of an energetic barrier at the interface between filament and ITO surface.

The long-term measurements of an identical functionalized cantilever open up the possibility to study the inherent statistical nature of diffusive switching. For this purpose, a long-term characterization on Au was conducted. Figure 2d depicts 100 consecutive cycles among the long-term measurement. It becomes apparent, that SET and RESET events are not triggered by fixed threshold voltages, but underlie a certain degree of stochasticity. Although great effort was invested to engineer filamentary systems with minimized switching variability, it is difficult to suppress it completely. Therefore, a deeper understanding of the statistical nature is inevitable. In Fig. 3a, all four threshold voltages per cycle (SET and RESET at either polarities) are

plotted against cycle number. A notable observation is, that the evolution of threshold voltages shows a significant trend ranging over hundreds of cycles in some regimes (highlighted as high correlation in the plot). However, in other regimes (highlighted as low correlation), the threshold voltages are subject to strong randomness. This observation suggests that there is partially a correlation in the switching characteristics in consecutive cycles and that the degree of correlation varies over the long-term measurement. To elucidate this, the linear correlation in the switching statistics was quantified by means of the Pearson coefficient. For both indicated regimes, the individual threshold voltages were related to the respective former value from the cycle before. This quantification is visualized in Figs. 3b and 3d for SET and RESET voltages with respect to positive polarity in the high correlation regime, respectively, and in Figs. 3c and 3e for the same characteristic voltages but in the low correlation regime. The values for the Pearson coefficient amount to 0.879 and 0.889 for SET and RESET in the high correlation regime, respectively, whereas they are 0.435 and 0.581 for SET and RESET in the low correlation regime, respectively. This supports the observation, that the threshold voltages are not statistically independent on each other, but are subject to correlations in the switching dynamics, which puts fundamental constraints in the design of real devices.

3   Noble Metal Alloy Nanoparticles for Diffusive Switching

An interesting approach to confine memristive action to the nanoscale lies in the transition from conventional bulk planar active electrodes towards nanostructured active electrodes or NPs. Using nanostructured electrodes (e.g. nanocones) showed a beneficial effect on the switching uniformity in Cu-based filamentary memristive devices [31]. NPs have recently attracted attention as building blocks for memristive switching devices and are readily employed, either to enhance the reproducibility by tailoring the electrical field inside the dielectric layer [32] or to act as a source of mobile metallic cations [8, 33]. Using AgAu and AgPt alloy NPs, the benefits of predefined electrical field enhancement and restricted mobile cation reservoirs were combined, and diffusive memristive action was studied at different length scales, ranging from individual NPs to multistack nanocomposites. Restriction of the mobile species reservoir is crucial to achieve stable diffusive switching as the formation of non-volatile filaments is inseparably linked to larger mass transport of the mobile species. The use of bimetallic NPs is particularly promising, because the amount of mobile species at the switching location can be effectively limited through NP composition and size [33]. Figure 4 gives an overview of different device setups which were studied in this context. AgPt and AgAu-NPs fabricated from a Haberland-type gas aggregation source serve as fundamental memristive building units. To obtain alloy NPs such as AgAu or AgPt, the concept of gas phase synthesis in a magnetron-based Haberland-type gas aggregation source [34–36] was expanded by the introduction of the multicomponent target approach. Here, instead of a planar bulk target, a custom-made target is applied, which consists of a Ag target with a
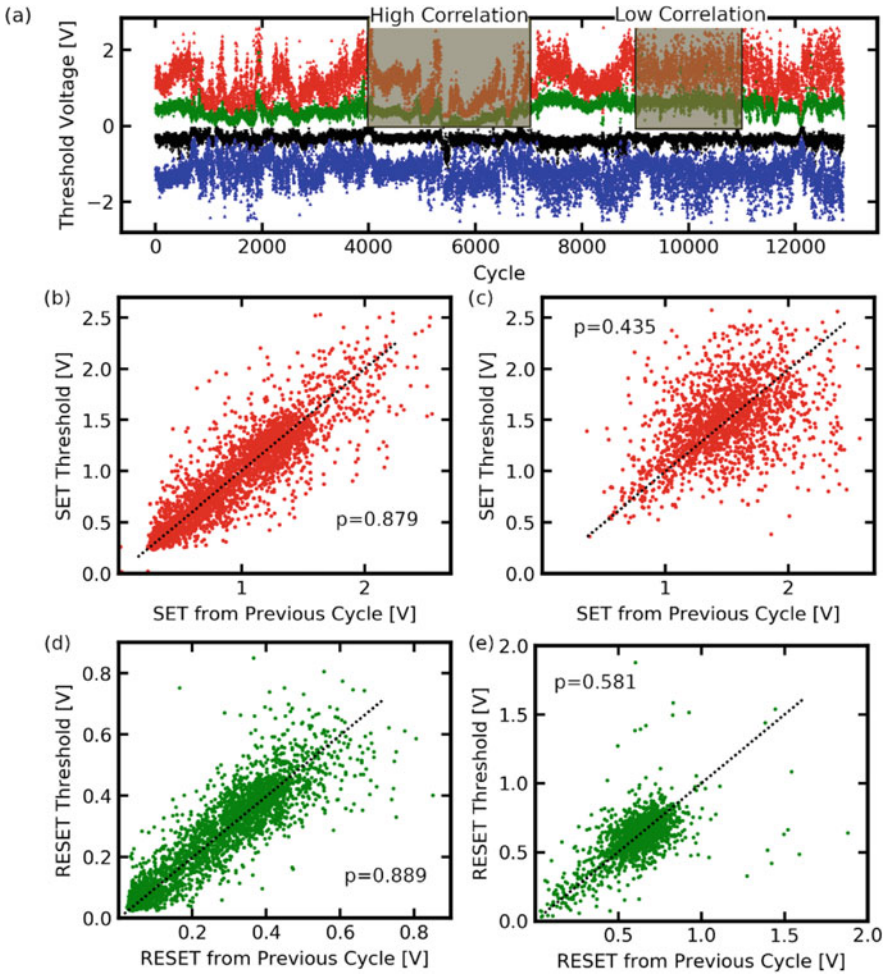
Fig. 3 Switching statistics extracted from the long-term measurement of a Ag/Si$_3$N$_4$ system on Au. **a** Characteristic threshold voltages (SET (red) and RESET (green) at positive polarity, SET (blue) and RESET (black) at negative polarity) plotted versus cycle number. Two regimes are highlighted: One showing systematic trends in the evolution of threshold voltages (labeled as high correlation) and one showing strong randomness (low correlation). The linear correlation was quantified by the Pearson coefficient in both regimes by relating the individual threshold voltages to the respective former value from the cycle before for SET and RESET in the high correlation regime (**b**, **d**) and SET and RESET in the low correlation regime (**c**, **e**). Reproduced under CC-BY 4.0 license from [28]
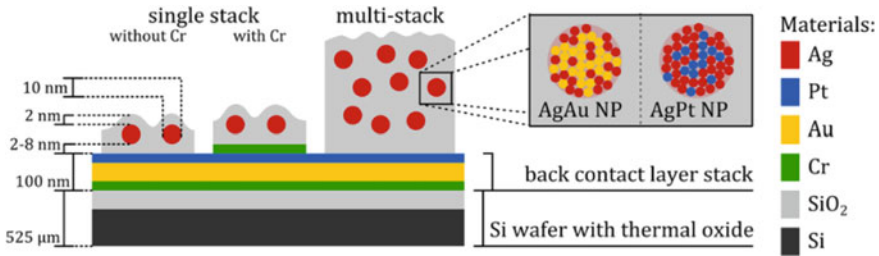
Fig. 4 Device setups under investigation. AgAu and AgPt-NPs act as fundamental memristive building units and are encapsulated into SiO_2 for a complete ECM-based memristive device. Left: Experimental setup to test the switching performance of individual NPs via cAFM. Right: The upscaling capabilities of the NP-based approach was tested on multiple stacks of NPs and SiO_2 layers via a macroscopic probe. Reproduced under CC-BY 4.0 license from [33]

trench and embedded Au or Pt wires. Using this methodology, the material usage of the more precious metal was significantly enhanced and the NP alloy composition can be tailored and controlled *in-operando*. More details regarding the NP deposition methodology can be found elsewhere [35, 36]. Encapsulation of the alloy NPs in a dielectric layer consisting of SiO_2 (deposited by reactive pulsed DC sputtering from a Si target in the presence of an Ar/O_2 atmosphere) completes the memristive device setup.

In contrast to the vast majority of ECM-based devices, the reservoir of active species (Ag in this case) has not the form of a continuous electrode, but is embedded into a dielectric layer between two inert electrodes. A major focus of this study was to explore the scalability of this concept which is one key aspect concerning device implementation. Therefore, this concept was tested on two different scales: Firstly, the switching performance of an individual alloy NP was tested via cAFM, which embodies the lowest limit of the scalability range. Secondly, macroscopic devices consisting of multiple stacks of NPs and SiO_2 layers were fabricated to characterize the upscaling capabilities.

The NP-based approach used to implement memristive devices on the nanoscale offers several advantages. The location of NPs inside the dielectric layer efficiently predefines the path where the filament is formed, which is essential for the device integration on the lower nanoscale. The strong localization of memristive action is additionally enhanced by the inherent electrical field concentration at the surface of a NP. Since the mechanisms leading to filament formation are driven by electrical fields, a substantial facilitation of memristive switching by using NPs is expected. Further, application of alloy NPs instead of the elemental counterparts provides additional degrees of freedom to tune the memristive action. For the alloy system presented here, AgAu and AgPt, Ag is the active species, whereas to more noble component, Au or Pt, is completely inert and will remain at its location inside the dielectric layer, which is expected to facilitate the long-term anchoring of the filament path.

To understand the memristive action of alloy NPs as building block for memristive devices, first the switching at the level on an individual NP has to be understood.
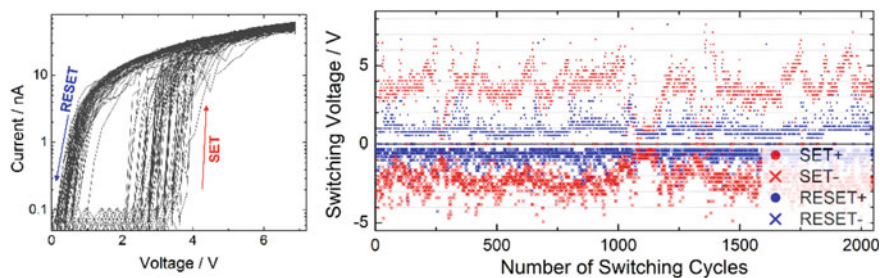
Fig. 5 Essential results from the memristive performance characterization of a single AgPt-NP encapsulated in SiO_2 via voltage sweeps between -7 and $+7$ V probed by cAFM. **a** shows a plot of 70 consecutive cycles which are representative for the diffusive switching behavior of a single NP. **b** shows the threshold voltage statistics for over 2000 consecutive cycles. Adapted under CC-BY 4.0 license from [33]

For this purpose, a stacked system consisting AgPt-NPs encapsulated in SiO_2 was prepared through consecutive deposition steps of 8 nm SiO_2, AgPt-NPs at sparse filling factor and 2 nm SiO_2. A cAFM setup was applied to identify the position of a NP and to measure the current response at the location of an individual AgPt-NP via driving voltage sweeps between -7 and $+7$ V through the conductive tip, while the common Au thin film served as back electrode. A serial resistance of 101 MΩ was applied to this measurement to limit the current flowing through the system. In this measurement, stable diffusive memristive switching was observed for over 2000 cycles. Essential results of the measurement are depicted in Fig. 5.

The memristive behavior of the single AgPt-NP matches diffusive switching and consequently follows the identical qualitative characteristics as described for single filament switching in the previous section. This is represented in Fig. 5a, where 70 consecutive cycles among the measurement are plotted. The threshold voltage statistics for over 2000 consecutive cycles are given in Fig. 5b. Also in the case of NPs, the switching characteristics underlie a considerable degree of stochasticity. Interestingly, no initial electroforming step had to be performed to achieve a stable switching regime. The origin of the diffusive switching behavior in the single AgPt-NP system is not merely determined by the external current limitation (like in the functionalized cantilever devices in the previous section), but rather by the absence of bulk Ag electrodes. The alloy NP approach allows for a severe limitation of the Ag amount (i.e. by small NP diameter or low ratio between Ag and noble alloy component) and therefore provides degrees of freedom to constrain the system into diffusive switching regime by supplying not enough Ag to build a non-volatile filament.

Further, the scalability of the NP-based approach was tested through studies on macroscopic devices. For this purpose, samples consisting of multiple stacks of SiO_2 layers and either AgAu or AgPt-NPs were fabricated and characterized in analogy to the cAFM measurements. To account for effects arising from the thickness of the SiO_2 separation layer, an effective SiO_2 thickness of 2 nm between the NP depositions was chosen for the AgAu sample whereas it was chosen as 4 nm for the

AgPt sample. A soft Pt probe having a diameter of 125 μm was applied to contact the samples. The samples were stressed again via voltage sweeps under current limitation with a 1 MΩ serial resistor. Figure 6a and 6b exhibit the current responses and threshold switching statistics measured for the macroscopic devices based on AgAu or AgPt-NPs, respectively. Generally, it can be observed, that the diffusive switching characteristics as known from a single NP is preserved, although multiple switching junctions inside the sample are expected to contribute to the filament formation. Comparison of the different alloy systems show, that the HRS of the AgAu sample allows a measurable conduction whereas the HRS of the AgPt sample is hidden in the noise level of the experimental instrumentation. These observations could be connected to the different thicknesses of the SiO$_2$ separation layer. In the AgAu sample, the lower SiO$_2$ thickness possibly allows significant leakage currents whereas the 4 nm SiO$_2$ layer thickness in the AgPt sample results in effective insulation.
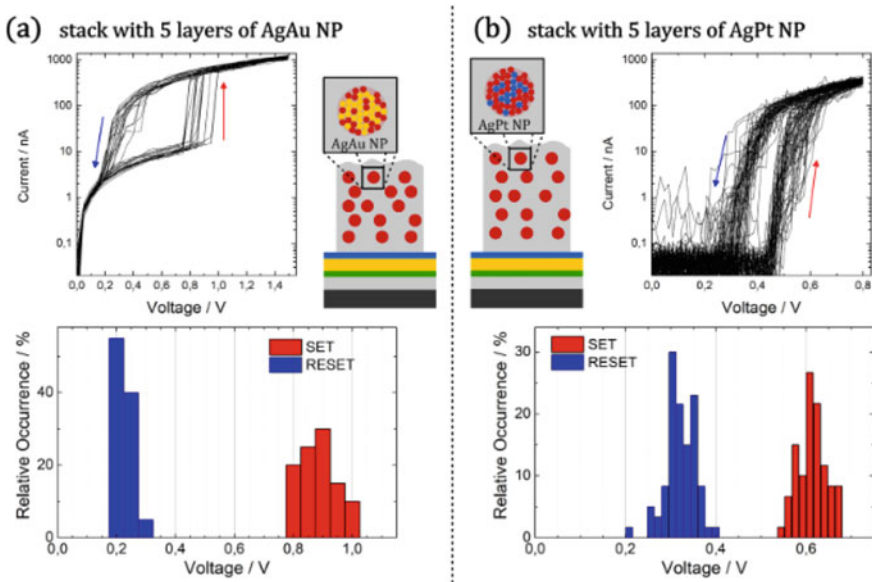

Fig. 6 Upscaling of the NP-based approach. Macroscopic devices were fabricated by multiple stacking of SiO$_2$ layers and AgPt or AgAu-NPs. The samples were contacted by a macroscopic Pt probe (diameter of 125 μm) and characterized via voltage sweeps. **a** and **b** show switching cycles at positive bias and extracted switching statistics for systems with AgAu and AgPt-NPs, respectively. Reproduced under CC-BY 4.0 license from [33]

4 Distributed Ag-Based NP Switching in Memristive Networks

Alongside with the profound characterization and device engineering of single memristors, further sophisticated challenges arise from the question how to build functional networks with a magnitude of memristive switching units. These challenges can be tackled by two different paradigms: Either by a regular and precisely engineered arrangement of hardwired memristive devices, like it is done in cross-bar arrays, or by reliance on self-assembly mechanisms to achieve a random dispersion of memristive switching units throughout a network. In the last section, two strategies for the fabrication of Ag-NP based memristive switch networks under self-assembly principles will be discussed.

4.1 Sparse CNT Networks with Implanted AgAu Nanoparticles

From investigating single NPs or vertical stacks of only a few NPs, in this section, the transition of NP-based memristive switching to the horizontal orientation is discussed. For achieving the nanoscaled distances required for memristive switching phenomena vertically, a variety of thin film deposition techniques are already well established. However, in a lateral orientation only sophisticated techniques like e-beam lithography [37, 38] offer the necessary resolution to produce nanoscaled gaps between electrodes, that allow for memristive switching. In this section, a new approach for the fabrication of lateral nanogaps as well as the memristive switching, when combined with bimetallic NPs described in the previous section, is discussed [39].

This approach is based on depositing carbon nanotubes (CNTs) between electrodes fabricated by conventional UV-lithography where the spacing between the electrodes is of several micrometers. The deposition is controlled such, that the CNTs form a sparse network and a subsequent Joule heating step removes any existing conductive pathways between the electrodes. The network then exhibits nanoscaled gaps between CNTs allowing for memristive switching phenomena. To fulfill its expected functionality, the CNT network has to meet certain requirements:

- The network must fill the space between the electrodes, so that all electrodes are in electrical contact with the CNT network.
- The CNTs must be finely dispersed, so that there are no dense agglomerations of CNTs, as those would impede the subsequent Joule heating step.
- The network must be below the percolation point but dense enough, so that the distance between individual tubes is in the nanometer range.

- The CNTs must not be heavily coated by surfactants or other additives, which would hinder removing short-circuiting paths during the Joule heating step.

Based on these requirements, a custom-made CNT dispersion has been developed by mixing ethanol with dry, pristine CNTs and a small amount of PEDOT:PSS. The mixture has been ultra-sonicated with a high-power sonicator to break up the CNT bundles and disperse them, whereas the PEDOT:PSS prevented a re-agglomeration of the CNTs and kept them finely dispersed. Despite the PEDOT:PSS acting as a surfactant, the low amount used is not detrimental to the Joule heating step. Using ethanol as a solvent allowed for a quick spin coating deposition in which single drops of dispersion are dropped subsequently onto the substrate under constant rotation, making the density of CNTs in the network well controllable. A sparse network of CNTs is shown in Fig. 7a. Conductive pathways in the CNT network, which have been short-circuiting the electrodes, were removed via Joule heating by applying voltages of up to 30 V.

AgAu NPs have been deposited onto the CNT networks with a Haberland-type gas aggregation source, which has been discussed in the previous section. The percolation point of the NPs deposition process has been determined by *in-operando* current measurements. It has been used to adjust the NP density to be just below the percolation point, so that the distances between particles are in the lower nanometer range, which is indicated in Fig. 7b. CNT networks with implanted AgAu NPs showed ECM-type memristive switching with a switching behavior exhibiting a hybrid of diffusive and bipolar characteristics. Current–voltage measurements are shown in Fig. 7c and d. Figure 7c depicts the diffusive switching mode, where the LRS is reset to the HRS when falling below a voltage threshold (cf. Figure 5). Additionally, Fig. 7d shows the capabilities for resetting the resistance state when cycled quickly into the reverse voltage regime, which is a feature of bipolar memristors.

A time resolved current measurement is shown in Fig. 7e, which indicates the retention time i.e. the time until the HRS is reached after reducing the applied voltage. Below the voltage threshold, diffusion and surface tension lead to a collapse of the silver filament. However, the thickness of the filament, and thus the amount of silver in it, defines its lifetime [13]. Therefore, it is proposed that the deposited NPs provide a limited silver reservoir for filament formation. The amount of silver atoms is limited such that no stable filament can be formed. But there is still sufficient silver to form filaments that are thick enough to show a substantial lifetime.

The retention time can also be described as the "memory span" of the device, as it remembers its resistance state. While in non-volatile memory applications, the retention time is supposed to be as high as possible to prevent data loss, a second-scale retention can be used for a short-term memory effect. Short-term memories are an efficient way of storing information that is only required for a limited amount of time, as it automatically forgets that information by itself again and thus does not have to be explicitly reset.
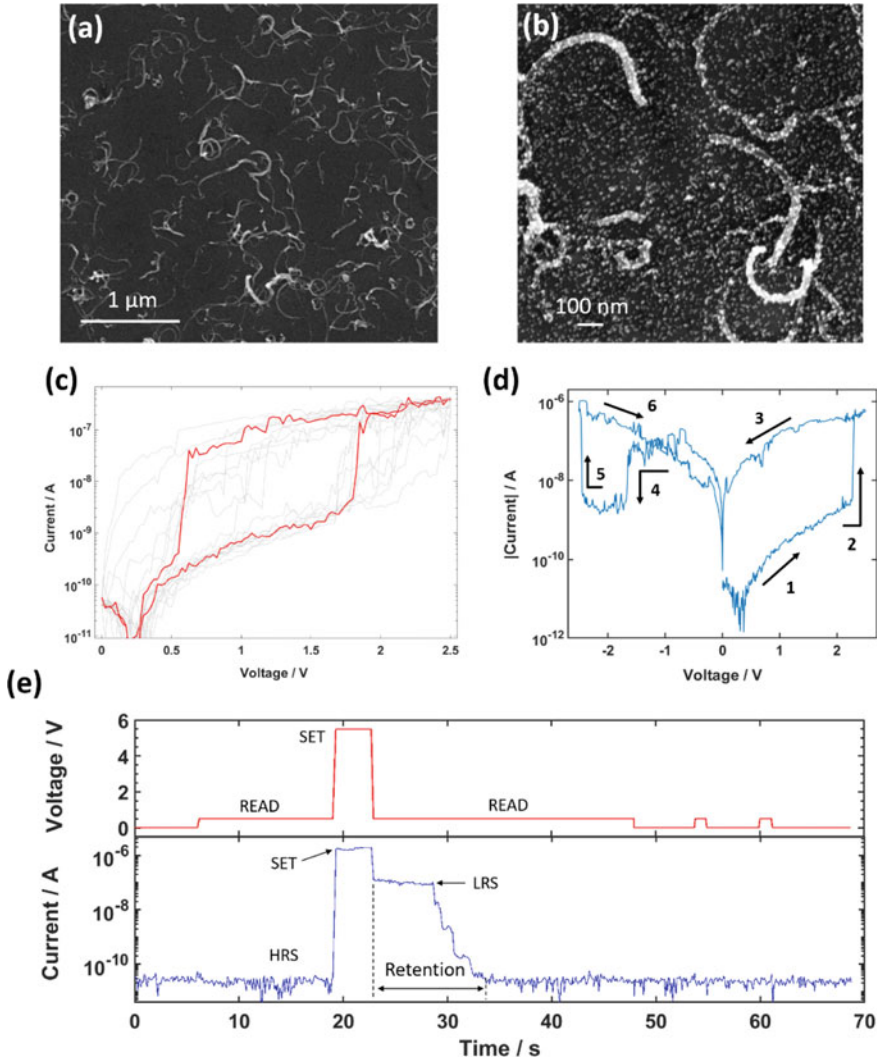
Fig. 7 Morphology and switching behavior of CNT networks with implanted AgAu NPs. **a** + **b** SEM micrographs of sparse CNT networks without **a** and with **b** deposited AgAu NPs. **c** Current–voltage cycles of a CNT network with NPs showing diffusive memristive switching behavior. **d** A current–voltage cycle showing the bipolar reset mechanism by applying reverse voltages (see arrow 4). **e** Time-resolved current measurement showing the retention of the LRS. Adapted under CC-BY 4.0 license from [39]

4.2   Nanoparticle Networks

In addition to the networks of the previous section, another approach for large-scale memristive switch network implementation, which solely makes use of metallic NPs for building the network, is discussed in this section. Elemental Ag-NPs synthesized from Haberland-type gas aggregation source, which are similar to the memristive bimetallic Ag-based NPs as discussed in Sect. 3, are applied as fundamental memristive building units in this type of network. Network formation is done by random assembly (realized by the statistical nature of the deposition process) of the Ag-NPs between chemically inert electrodes. The resulting network consists of a complex arrangement of clusters of electrically connected Ag-NPs and potential switching gaps between different clusters. The system scale is defined by the electrode separation and can be easily set to large-scale systems in horizontal electrode geometry. A NP network system with maximized complexity (in terms of maximized amount of metastable network configurations) can be realized through careful tuning of the NP filling factor at the percolation transition [24]. A schematic setup of a percolated NP network is shown in Fig. 8a. In the subcritical regime, no network response is possible, because of missing current paths having the scale of the overall system. In addition to that, in the supercritical regime, the network complexity is expected to be strongly reduced due to the existence of stable current paths that dominate the network response. However, it should be noted that NP networks in the supercritical regime potentially are still able to show a dynamic response which results from the reconfiguration of interface defects (such as grain boundaries) between connected NPs, as it is reported for Au-NP networks above the percolation threshold [17]. Exactly at the percolation threshold, which marks the critical regime of a phase transition, the network configuration is located at some point between none and full connectivity and allows for ongoing transitions between a multitude of different metastable network configurations [40]. Figure 8b shows schematically a Ag-NP network under indication of potential switching gaps. The state of the network is accessed by the conductance between both electrodes, which is determined by the configuration of all switching gaps across the network. Upon an external disturbance, e.g. application of voltage stimuli across the electrodes, localized memristive switching at individual switching gaps may be triggered, which lead to a redistribution of potential differences across other switching gaps. As a consequence, memristive switching at a certain location could induce switching at other gaps in the network, resulting in a complex interplay of switching gaps distributed over the whole network. Figure 8c depicts the network response of a percolated Ag-NP network to a DC bias of 5 V. It can be seen, that the network dynamics are governed by ongoing transitions between a multitude of metastable conductance states over more than 1 h of operation. There is no indication that the network converges to a definable conductance state, which is in contrast to the lower-scale vertical NP-based devices in Sect. 3. Figure 8d shows the probability density of the observed conductance states for the vertical AgPt-NP devices from Sect. 3 (cf. Figure 6, right) and the percolated Ag-NP network. This comparison stresses out, that for the small-scale NP-based memristive devices well

differentiable conductance states (i.e. LRS and HRS) dominate the operation, which is not the case for the large-scale NP network. Instead, for the percolated NP network, the well differentiable conductance states are fading, which can be seen as an indicator for collective behavior of a multitude of switching junctions. Such a behavior is potentially interesting for neuromorphic computational concepts like reservoir computing, which require complex networks of interacting non-linear elements able to map input information into temporal dynamics in the network [41].

Fig. 8 Behavior of networks comprised of Ag-NPs and poised at the percolation threshold. **a** A schematic percolation curve showing classification of the network states into sub- and supercritical and critical regime depending on the filling factor. **b** is showing schematically a critical network state, where no global connectivity persists, but the network state is defined by the configuration of a multitude of switching gaps. **c** exhibits the network response upon application of a constant external bias of 5 V. **d** shows the distribution of distinct resistive states for a AgPt-multistack device as discussed in Sect. 3 (left) and extracted from the Ag-NP network response shown in (**c**) (right)
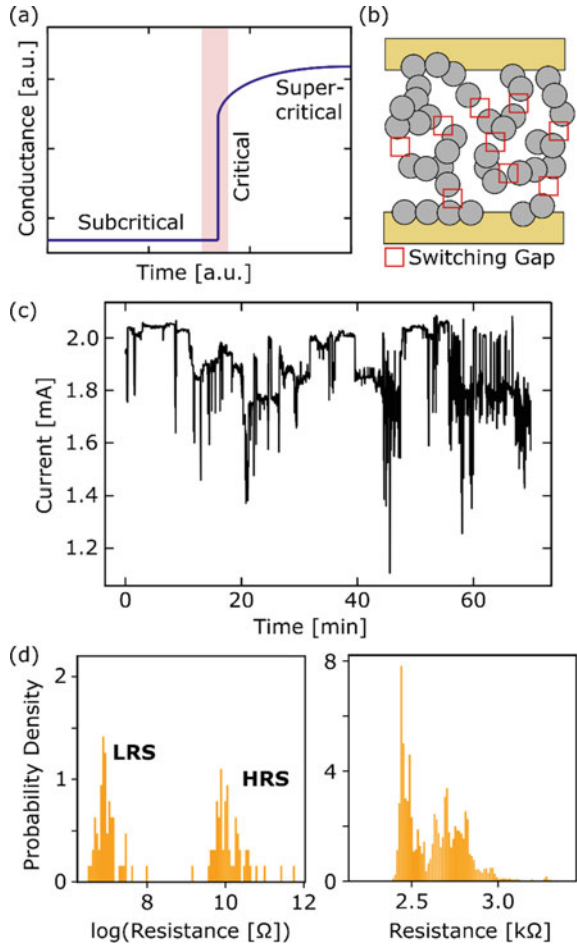
5   Conclusion

In this chapter, Ag-mediated reconfiguration of resistance states have been observed throughout different device implementations and system scales, ranging from individual filaments to complex assemblies of switching gaps. Fundamental research into the long-term switching dynamics of an individual Ag-filament via cAFM can be considerably facilitated through direct implementation of the memristive material system at the cantilever apex instead of conventional contacting, because it mitigates loss in data significance by thermal drift effects. This approach was exploited to study the cycle-to-cycle variability of filamentary diffusive switching dynamics. It was observed that the variability in the switching dynamics of an individual filament cannot be seen as purely stochastic, but potential correlation effects must be taken into account. Further, AgAu and AgPt alloy NPs have been found to be promising and versatile building blocks for diffusive memristive devices with a broad range of switching properties. Investigations via cAFM on individual Ag-based alloy NPs have shown, that already a single NP can act as a fundamental memristive building unit. Application of NPs for memristive devices opens up several design opportunities, such as inherent field enhancement at the surface of the NP, high localization of the memristive action at the location of the NP in contrast to bulk electrodes and precise regulation of the number of active species through NP size and composition, which is important to stabilize the diffusive switching regime of the device. Finally, two approaches to build large-scale memristive switch networks by self-assembly principles with a different degree of sparseness are discussed. The first approach is comprised of a sparse CNT network, which establishes a static network topology, and AgAu-NPs, which enable memristive switching between adjacent CNT sites in the network. Such hybrid CNT/AgAu-NPs networks were shown to exhibit a mixed form of diffusive and bipolar switching. The second approach treats networks only comprised of Ag-NP with a filling factor around the percolation threshold. The Ag-NP networks differ from their lower-scale counterparts regarding the non-existence of stable and definable conductance states. Instead of a clear differentiation into LRS or HRS, the networks dynamics of percolated Ag-NP networks are governed by ongoing transitions between a multitude of metastable states, which makes them interesting for neuromorphic computation schemes, where spatio-temporal mapping of information into complex patterns is required.

References

1. Jeong, D.S., Kim, K.M., Kim, S., Choi, B.J., Hwang, C.S.: Memristors for energy-efficient new computing paradigms. Adv. Electron. Mater. **2**, 1–27 (2016). https://doi.org/10.1002/aelm.201600090

2. Kendall, J.D., Kumar, S.: The building blocks of a brain-inspired computer. Appl. Phys. Rev. **7** (2020).https://doi.org/10.1063/1.5129306

3. Zhang, T., Yang, K., Xu, X., Cai, Y., Yang, Y., Huang, R.: Memristive devices and networks for brain-inspired computing. Phys. Status Solidi - Rapid Res. Lett. **13**, 1–21 (2019). https://doi.org/10.1002/pssr.201900029

4. Yang, J.Q., Wang, R., Ren, Y., Mao, J.Y., Wang, Z.P., Zhou, Y., Han, S.T.: Neuromorphic engineering: from biological to spike-based hardware nervous systems. Adv. Mater. **32**, 1–32 (2020). https://doi.org/10.1002/adma.202003610

5. Zidan, M.A., Strachan, J.P., Lu, W.D.: The future of electronics based on memristive systems. Nat. Electron. **1**, 22–29 (2018). https://doi.org/10.1038/s41928-017-0006-8

6. Vahl, A., Carstensen, J., Kaps, S., Lupan, O., Strunskus, T., Adelung, R., Faupel, F.: Concept and modelling of memsensors as two terminal devices with enhanced capabilities in neuromorphic engineering. Sci. Rep. **9**, 1–9 (2019). https://doi.org/10.1038/s41598-019-39008-5

7. Wang, J., Zhuge, F.: Memristive synapses for brain-inspired computing. Adv. Mater. Technol. **4**, 1–20 (2019). https://doi.org/10.1002/admt.201800544

8. Wang, Z., Joshi, S., Savel'ev, S.E., Jiang, H., Midya, R., Lin, P., Hu, M., Ge, N., Strachan, J.P., Li, Z., et al.: Memristors with diffusive dynamics as synaptic emulators for neuromorphic computing. Nat. Mater. **16**, 101–108 (2017). https://doi.org/10.1038/nmat4756

9. Midya, R., Wang, Z., Asapu, S., Joshi, S., Li, Y., Zhuo, Y., Song, W., Jiang, H., Upadhay, N., Rao, M., et al.: Artificial Neural Network (ANN) to Spiking Neural Network (SNN) converters based on diffusive memristors. Adv. Electron. Mater. **5**, 1–7 (2019). https://doi.org/10.1002/aelm.201900060

10. Lim, E.W., Ismail, R.: Conduction mechanism of valence change resistive switching memory: a survey. Electron. **4**, 586–613 (2015). https://doi.org/10.3390/electronics4030586

11. Edwards, A.H., Barnaby, H.J., Campbell, K.A., Kozicki, M.N., Liu, W., Marinella, M.J.: Reconfigurable memristive device technologies. Proc. IEEE **103**, 1004–1033 (2015). https://doi.org/10.1109/JPROC.2015.2441752

12. Cha, J.H., Yang, S.Y., Oh, J., Choi, S., Park, S., Jang, B.C., Ahn, W., Choi, S.Y.: Conductive-bridging random-access memories for emerging neuromorphic computing. Nanoscale **12**, 14339–14368 (2020). https://doi.org/10.1039/d0nr01671c

13. Wang, W., Wang, M., Ambrosi, E., Bricalli, A., Laudato, M., Sun, Z., Chen, X., Ielmini, D.: Surface diffusion-limited lifetime of silver and copper nanofilaments in resistive switching devices. Nat. Commun. **10**, 1–9 (2019). https://doi.org/10.1038/s41467-018-07979-0

14. Wang, Z., Rao, M., Midya, R., Joshi, S., Jiang, H., Lin, P., Song, W., Asapu, S., Zhuo, Y., Li, C., et al.: Threshold switching of Ag or Cu in dielectrics: materials, mechanism, and applications. Adv. Funct. Mater. **28**, 1–19 (2018). https://doi.org/10.1002/adfm.201704862

15. Jiang, H., Belkin, D., Savel'Ev, S.E., Lin, S., Wang, Z., Li, Y., Joshi, S., Midya, R., Li, C., Rao, M., et al.: A novel true random number generator based on a stochastic diffusive memristor. Nat. Commun. **8** (2017). https://doi.org/10.1038/s41467-017-00869-x

16. Minnai, C., Bellacicca, A., Brown, S.A., Milani, P.: Facile fabrication of complex networks of memristive devices. Sci. Rep. **7**, 1–8 (2017). https://doi.org/10.1038/s41598-017-08244-y

17. Mirigliano, M., Decastri, D., Pullia, A., Dellasega, D., Casu, A., Falqui, A., Milani, P.: Complex electrical spiking activity in resistive switching nanostructured Au two-terminal devices. Nanotechnology **31** (2020). https://doi.org/10.1088/1361-6528/ab76ec

18. Bose, S.K., Mallinson, J.B., Gazoni, R.M., Brown, S.A.: Stable self-assembled atomic-switch networks for neuromorphic applications **64** (2017), 5194–5201

19. Stieg, A.Z., Avizienis, A.V., Sillin, H.O., Martin-Olmos, C., Aono, M., Gimzewski, J.K.: Emergent criticality in complex turing B-type atomic switch networks. Adv. Mater. **24**, 286–293 (2012). https://doi.org/10.1002/adma.201103053

20. Sillin, H.O., Aguilera, R., Shieh, H.H., Avizienis, A.V., Aono, M., Stieg, A.Z., Gimzewski, J.K.: A theoretical and experimental study of neuromorphic atomic switch networks for reservoir computing. Nanotechnology **24** (2013). https://doi.org/10.1088/0957-4484/24/38/384004

21. Du, C., Cai, F., Zidan, M.A., Ma, W., Lee, S.H., Lu, W.D.: Reservoir computing using dynamic memristors for temporal information processing. Nat. Commun. **8**, 1–10 (2017). https://doi.org/10.1038/s41467-017-02337-y

22. Pike, M.D., Bose, S.K., Mallinson, J.B., Acharya, S.K., Shirai, S., Galli, E., Weddell, S.J., Bones, P.J., Arnold, M.D., Brown, S.A.: Atomic scale dynamics drive brain-like avalanches in percolating nanostructured networks. Nano Lett. **20**, 3935–3942 (2020). https://doi.org/10.1021/acs.nanolett.0c01096

23. Shirai, S., Acharya, S.K., Bose, S.K., Mallinson, J.B., Galli, E., Pike, M.D., Arnold, M.D., Brown, S.A.: Long-range temporal correlations in scale-free neuromorphic networks. Netw. Neurosci. **4**, 432–447 (2019). https://doi.org/10.1162/netn_a_00128

24. Mallinson, J.B., Shirai, S., Acharya, S.K., Bose, S.K., Galli, E., Brown, S.A.: Avalanches and criticality in self-organized nanoscale networks. Sci. Adv. **5**, eaaw8438 (2019). https://doi.org/10.1126/sciadv.aaw8438

25. Chekol, S.A., Menzel, S., Ahmad, R.W., Waser, R., Hoffmann-Eifert, S.: Effect of the threshold kinetics on the filament relaxation behavior of ag-based diffusive memristors. Adv. Funct. Mater. **32** (2022). https://doi.org/10.1002/adfm.202111242

26. Valov, I.; Waser, R.; Jameson, J.R.; Kozicki, M.N. Erratum: Electrochemical metallization memories—fundamentals, applications, prospects. Nanotechnology **22** (2011).https://doi.org/10.1088/0957-4484/22/28/289502

27. Yang, Y., Huang, R.: Probing memristive switching in nanoionic devices. Nat. Electron. **1**, 274–287 (2018). https://doi.org/10.1038/s41928-018-0069-1

28. Carstens, N., Vahl, A., Gronenberg, O., Strunskus, T., Kienle, L., Faupel, F., Hassanien, A.: Enhancing reliability of studies on single filament memristive switching via an unconventional cafm approach. Nanomaterials **11**, 1–16 (2021). https://doi.org/10.3390/nano11020265

29. Ke, J.J., Wei, T.C., Tsai, D.S., Lin, C.H., He, J.H.: Surface effects of electrode-dependent switching behavior of resistive random-access memory. Appl. Phys. Lett. **109** (2016).https://doi.org/10.1063/1.4963671

30. Lübben, M., Menzel, S., Park, S.G., Waser, R., Valov, I.: SET kinetics of electrochemical metallization cells: influence of counter-electrodes in SiO_2/Ag based systems. Nanotechnology **28** (2017)

31. Kim, H.J., Park, T.H., Yoon, K.J., Seong, W.M., Jeon, J.W., Kwon, Y.J., Kim, Y., Kwon, D.E., Kim, G.S., Ha, T.J., et al.: Fabrication of a Cu-Cone-Shaped cation source inserted conductive bridge random access memory and its improved switching reliability. Adv. Funct. Mater. **29**, 1–13 (2019). https://doi.org/10.1002/adfm.201806278

32. Choi, B.J., Torrezan, A.C., Norris, K.J., Miao, F., Strachan, J.P., Zhang, M.X., Ohlberg, D.A.A., Kobayashi, N.P., Yang, J.J., Williams, R.S.: Electrical performance and scalability of Pt dispersed SiO_2 nanometallic resistance switch. Nano Lett. **13**, 3213–3217 (2013). https://doi.org/10.1021/nl401283q

33. Vahl, A., Carstens, N., Strunskus, T., Faupel, F., Hassanien, A.: Diffusive memristive switching on the nanoscale, from individual nanoparticles towards scalable nanocomposite devices. Sci. Rep. **9**, 1–10 (2019). https://doi.org/10.1038/s41598-019-53720-2

34. Haberland, H., Karrais, M., Mall, M., Thurner, Y.: Thin films from energetic cluster impact: a feasibility study. J. Vac. Sci. Technol. A Vacuum, Surfaces, Film. **10**, 3266–3271 (1992). https://doi.org/10.1116/1.577853

35. Drewes, J., Vahl, A., Carstens, N., Faupel, F., Strunskus, T.: Enhancing composition control of alloy nanoparticles from gas aggregation source by in operando optical emission spectroscopy 1–11 (2021). https://doi.org/10.1002/ppap.202000208

36. Vahl, A., Strobel, J., Reichstein, W., Polonskyi, O., Strunskus, T., Kienle, L., Faupel, F.: Single target sputter deposition of alloy nanoparticles with adjustable composition via a gas aggregation cluster source. Nanotechnology **28**, (2017). https://doi.org/10.1088/1361-6528/aa66ef

37. Puzyrev, Y.S., Shen, X., Zhang, C.X., Hachtel, J., Ni, K., Choi, B.K., Zhang, E.X., Ovchinnikov, O., Schrimpf, R.D., Fleetwood, D.M., et al.: Memristive devices from ZnO nanowire bundles and meshes. Appl. Phys. Lett. **111**, (2017). https://doi.org/10.1063/1.5008265
38. Le, P.Y., Murdoch, B.J., Barlow, A.J., Holland, A.S., McCulloch, D.G., McConville, C.F., Partridge, J.G.: Electroformed, self-connected tin oxide nanoparticle networks for electronic reservoir computing. Adv. Electron. Mater. **6**, 1–7 (2020). https://doi.org/10.1002/aelm.202000081
39. Terasa, M.I., Holtz, P., Carstens, N., Kaps, S., Faupel, F., Vahl, A., Adelung, R.: Sparse CNT networks with implanted AgAu nanoparticles: a novel memristor with short-term memory bordering between diffusive and bipolar switching. PLoS One **17**, 1–12 (2022). https://doi.org/10.1371/journal.pone.0264846
40. Shew, W.L., Plenz, D.: The functional benefits of criticality in the cortex (2013).https://doi.org/10.1177/1073858412445487
41. Tanaka, G., Yamane, T., Benoit, J., Nakane, R., Kanazawa, N., Takeda, S., Numata, H., Nakano, D., Hirose, A.: Recent advances in physical reservoir computing: a review. Neural Netw. **115**, 100–123 (2019). https://doi.org/10.1016/j.neunet.2019.03.005